

Low temperature chemical vapor deposition of superconducting molybdenum carbonitride thin films

Elham Mohimi,¹ Kinsey Canova,¹ Zhejun Zhang,¹ Sumeng Liu,² Justin L. Mallek,³ Gregory S. Girolami,² and John R. Abelson^{1,a)}

¹Department of Materials Science and Engineering, University of Illinois at Urbana-Champaign, 1304 W. Green St., Urbana, Illinois 61801

²School of Chemical Sciences, University of Illinois at Urbana-Champaign, 600 South Mathews Avenue, Urbana, Illinois 61801

³MIT-Lincoln Laboratory, 244 Wood St., Lexington, Massachusetts 02421

(Received 3 November 2018; accepted 19 December 2018; published 9 January 2019)

Thin films of molybdenum carbonitride, MoC_xN_y , are deposited by low temperature chemical vapor deposition from $\text{Mo}(\text{CO})_6$ and NH_3 in the temperature range 150–300 °C. At a substrate temperature of 200 °C and $\text{Mo}(\text{CO})_6$ pressure of 0.01 mTorr, the composition varies from $\text{MoC}_{0.48}\text{N}_{0.20}$ to $\text{MoC}_{0.36}\text{N}_{0.33}$ (i.e., greater nitrogen and less carbon content) upon increasing the ammonia pressure from 0.3 to 3.3 mTorr. At a constant $\text{Mo}(\text{CO})_6$ pressure of 0.01 mTorr and an NH_3 pressure of 2 mTorr, the composition varies from $\text{MoC}_{0.50}\text{N}_{0.30}$ to $\text{MoC}_{0.12}\text{N}_{0.40}$ with increasing substrate temperature from 150 to 300 °C. Selected films grown at substrate temperatures of 150, 200, and 250 °C are superconducting with critical temperatures of 4.7, 4.5, and 5.2 K, respectively. Grazing incidence x-ray diffraction data indicate that the films are crystalline and isomorphous with the cubic phases of Mo_2N and Mo_2C . With a forward-directed flux of precursors toward the surface, film growth is highly conformal in microtrenches of aspect ratio 6, with step coverages of ~0.85 and 0.80 at growth temperatures of 150 and 200 °C, respectively. *Published by the AVS.*

<https://doi.org/10.1116/1.5079805>

I. INTRODUCTION

Molybdenum nitrides, carbides, and related ternary carbonitride alloys are widely used commercially as diffusion barriers,^{1,2} hard coatings,^{3–6} and catalysts^{7–10} due to their high chemical stability, mechanical hardness, and high electrical conductivity. In molybdenum nitride and carbide phases, the metal atoms are closely-packed and the nitrogen and carbon atoms are interstitial.¹¹ Many of these phases are superconducting; Table I summarizes some published results for superconducting MoN and MoC phases. The variability in superconducting critical transition temperature, T_c , reflects several factors, such as disorder in MoN phases and stoichiometric variations.

Molybdenum carbonitrides are often prepared by traditional high-temperature carbiding or nitriding methods. However, if the goal is to deposit uniformly-thick (i.e., conformal) films on topologically complex surfaces, such as is required for the coating or filling of high aspect ratio vias and trenches, then methods such as low temperature chemical vapor deposition (CVD) are necessary.²⁵ Thin films of MoC_xN_y , where $x=0.20–0.55$ and $y=0.10–0.47$, have previously been deposited by CVD at relatively high temperatures of 450–650 °C from the single-source precursor $\text{Mo}(\text{N}^t\text{Bu})_2(\text{NH}^t\text{Bu})_2$.²⁶ Films have also been deposited at much lower temperatures, 80–300 °C, by plasma enhanced atomic layer deposition (ALD) from $\text{Mo}(\text{N}^t\text{Bu})_2(\text{NMe}_2)_2$ with an H_2+N_2 plasma.²⁷ One of the latter films, having the composition $\text{MoC}_{0.45}\text{N}_{0.08}$, was superconducting with a T_c of 8.8 K. In a separate study, MoC_xN_y

films were grown from $\text{Mo}(\text{CO})_6$ and NH_3 at 350–800 °C, and amorphous Mo_xN films have been grown by ALD from these same precursors in the narrow range of 155–170 °C.²⁸ To date, there have been no demonstrations of the conformal deposition of MoC_xN_y films in deep features.

Here, we report thermal CVD of low resistivity crystalline molybdenum carbonitride films at substrate temperatures of 150–300 °C from the precursors $\text{Mo}(\text{CO})_6$ and NH_3 . Films grown at 150, 200, and 250 °C exhibit superconducting transition temperatures of 4.7, 4.5, and 5.5 K, respectively, with step coverages of 80%–85% in trenches of aspect ratio 6:1.

II. EXPERIMENT

Growth of molybdenum carbonitride films is performed in a cold wall high vacuum chamber described elsewhere.²⁹ The pressure of $\text{Mo}(\text{CO})_6$ is controlled by setting the temperature of the precursor reservoir in the range 20–40 °C; this precursor flows under its own vapor pressure (i.e., with no carrier gas) through the delivery tube, which is heated to 55 °C to avoid condensation of sublimed precursor. The $\text{Mo}(\text{CO})_6$ pressure in the chamber is 0.01–0.03 mTorr. Research grade NH_3 (99.9992%) is delivered through a separate gas line, regulated by a mass flow controller, to establish a partial pressure of 0.3–9.0 mTorr in the chamber. All the gas delivery lines are pointed toward the substrate. This forward-directed expansion of gases increases the number of molecules which impinge on the substrate, i.e., the total fluxes on the substrate are higher than those due to the isotropic chamber pressure. In addition, the forward-directed

^{a)}Electronic mail: abelson@illinois.edu

TABLE I. Reported superconducting molybdenum nitride and molybdenum carbide phases with structure, crystallinity, zero-field superconducting transition temperature T_c , and residual resistivity ratio (RRR), defined as the ratio of room temperature to low temperature resistivity. —, value not reported.

Phase	Structure	Crystallinity	T_c (K)	RRR	Reference
B1-MoN	Cubic	Single crystal	29.4 ^a	—	12
B1-MoN	Cubic	Polycrystalline	12	1.7	13
γ -Mo ₂ N	Cubic	Polycrystalline	6	0.8–1.0	14
γ -Mo ₂ N	Cubic	Polycrystalline	8	0.97	15
γ -Mo ₂ N	Cubic	Single crystal	4.5	43	16
δ -MoN	Hexagonal	Single crystal	12	3.3	16
δ -MoN	Hexagonal	Polycrystalline	4.0–12	—	17
δ -MoN	Hexagonal	Polycrystalline	15.1	—	18
η -Mo ₃ C ₂	Hexagonal	Polycrystalline	8.5	—	19
η -Mo ₂ C	Hexagonal	Polycrystalline	7.4–8.9	—	20
δ -MoC	Cubic	Polycrystalline	10.15–14.7	—	21
δ -MoC	Cubic	Polycrystalline	12	—	22
α -Mo ₂ C	Orthorhombic	Polycrystalline	6.0–7.3	—	20
α -Mo ₂ C	Orthorhombic	—	12.2	—	23
β -Mo ₂ C	Hexagonal	Polycrystalline	5.1–7.2	—	20
β -Mo ₂ C	Hexagonal	Single crystal	8.0	—	24

^aCalculated.

flux will ballistically transport reactants down the axis of a deep feature such as a trench; this effect greatly enhances the coverage conformality (see Sec. III).

The substrate is heated radiatively to a growth temperature (T_g) of 150–300 °C, as measured by a K-type thermocouple attached to the sample holder. Film composition and resistivity measurements are performed on 300 nm SiO_2/Si substrates. On a bare SiO_2 surface, there is a considerable nucleation barrier for the deposition of $\text{Mo}(\text{CO})_6$ in the presence of NH_3 . To eliminate this barrier (and therefore to eliminate a nucleation delay time), a metallic seed layer of 1–2 nm of vanadium nitride (VN) is grown on SiO_2 by CVD from tetrakis (dimethylamido) vanadium and ammonia at the same temperature subsequently used to grow MoC_xN_y . VN grows with essentially no nucleation barrier on SiO_2 due to the facile transamination reaction,³⁰ affording a large areal density of nucleation sites that coalesce into a very smooth initial layer. The root mean square (rms) roughness of a 1 nm thick VN film is 0.3 nm. Films grown on top of this layer tend to be smooth because the onset of growth roughening is minimized.^{31,32} The parallel conductance of the thin VN film is neglected in resistivity measurements. Microtrench samples of multiple aspect ratios, coated with a conformal VN seed layer as for the SiO_2 substrates, are used for step coverage measurements.

Film thickness and microstructure are determined from cross-sectional scanning electron microscopy (SEM) images. Compositional depth profiles are obtained by Auger electron spectroscopy (AES). Core level binding energy is measured by x-ray photoelectron spectroscopy (XPS) using aluminum K α radiation. In selected samples, 2 min of surface sputtering by 3 kV Ar^+ ions is used to remove surface contamination due to air exposure. Film crystallinity is evaluated by grazing incidence x-ray diffraction (GIXRD). Surface roughness is

measured by atomic force microscopy. Film resistivity is measured by the 4-point probe method down to 4 K.

III. RESULTS AND DISCUSSION

A. Film growth and composition

In the absence of ammonia, chemical vapor deposition from 0.01 mTorr of $\text{Mo}(\text{CO})_6$ on SiO_2 at 200 °C affords a molybdenum oxycarbide film at a growth rate of 8 nm/min. AES depth profile analysis of the film indicates that the composition is $\text{MoO}_{0.3}\text{C}_{0.7}$, which is consistent with previous reports of CVD from this precursor.^{33–35} When the film is grown under identical conditions but capped *in situ* with HfB_2 , the oxygen content is roughly the same as for the air-exposed sample. This result indicates that the oxygen content in the film originates mostly from carbonyl decomposition³⁶ and not from postgrowth air exposure.

In the presence of 0.3 mTorr of NH_3 , CVD from 0.01 mTorr of $\text{Mo}(\text{CO})_6$ at 200 °C results in a molybdenum carbonitride film, $\text{MoC}_{0.48}\text{N}_{0.2}$, at a growth rate of 1.3 nm/min with 4 at. % oxygen impurity. A high resolution XPS scan after 2 min of Ar^+ sputtering [spectra available in Supplementary Fig. S1 (Ref. 42)] shows the presence of carbon in aliphatic (284.6 eV) and carbidic (283.3 eV) states.²⁷ The nitrogen 1s peak position is consistent with the nitride state (397.3 eV).²⁶ The presence of carbon provides additional evidence that some of the carbonyl ligands decompose on the surface rather than desorb into the gas phase; it is, however, difficult to tell if carbidic states were produced during film growth or surface sputtering before XPS. Incorporation of nitrogen is the result of NH_3 dissociation during growth.^{37–39}

If the ammonia pressure is increased and other deposition conditions are left unchanged [i.e., 0.01 mTorr of $\text{Mo}(\text{CO})_6$ at 200 °C], the nitrogen content increases and the carbon content decreases (Fig. 1): Film composition is $\text{MoC}_{0.48}\text{N}_{0.20}$, $\text{MoC}_{0.44}\text{N}_{0.25}$, and $\text{MoC}_{0.36}\text{N}_{0.33}$ when the NH_3 pressure is 0.3, 1.3, and 3.3 mTorr, respectively. The oxygen content for

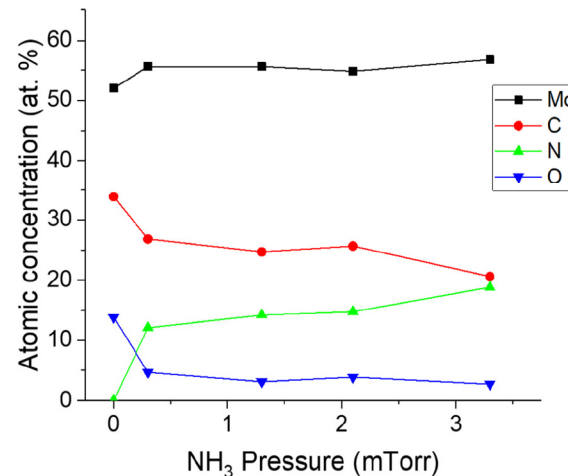


FIG. 1. Film composition vs NH_3 pressure at a constant growth temperature of 200 °C and an $\text{Mo}(\text{CO})_6$ pressure of 0.01 mTorr. For each sample, Auger sputter depth profiling reveals an essentially constant bulk composition, reported on the plot. Error in Auger data reduction is ± 1 at. %.

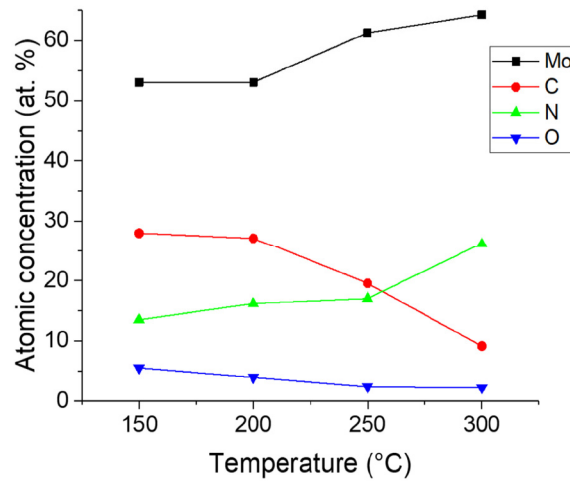


FIG. 2. Film composition vs temperature at constant $\text{Mo}(\text{CO})_6$ and NH_3 pressures of 0.01 and 2 mTorr, respectively. For each sample, Auger sputter depth profiling reveals an essentially constant bulk composition, reported on the plot. Error in Auger data reduction is ± 1 at. %.

all films remains relatively low at 3 at. %. The growth rate at 3.3 mTorr of NH_3 is 1 nm/min, smaller than the rate of 1.3 nm/min at 0.3 mTorr NH_3 . To explore the dependence of growth rate on NH_3 pressure more fully, experiments were conducted with 0.01 mTorr of $\text{Mo}(\text{CO})_6$ at 300 °C; the growth rate decreases from 3.0 to 0.3 nm/min when the NH_3 pressure is increased from 0.3 to 9 mTorr. The reason for this effect is not fully understood; it may reflect changes in the adsorption kinetics of reactants as the composition of the growth surface changes (a dynamic surface coverage or a poisoning effect); alternatively, the forward-directed component of the precursor flux may be partially scattered away from the substrate at higher ammonia pressures.

At higher temperatures, with 0.01 mTorr of $\text{Mo}(\text{CO})_6$ and 2 mTorr of NH_3 , the film becomes more N-rich and the O content decreases to <1 at. %: the composition is $\text{MoC}_{0.5}\text{N}_{0.3}$

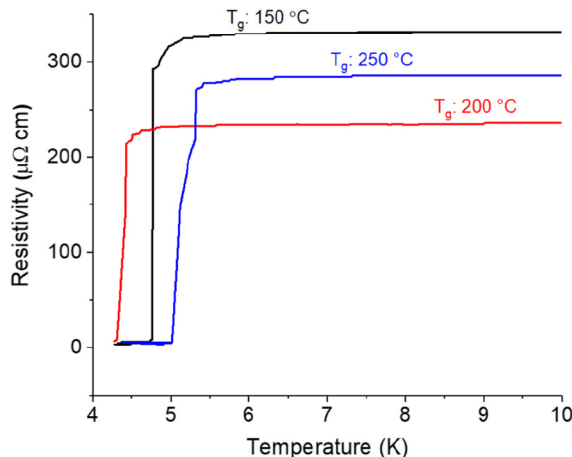


FIG. 3. Superconducting critical temperature of molybdenum carbonitride films grown at 150–250 °C from 0.01 mTorr of $\text{Mo}(\text{CO})_6$ and 0.7 (150 °C) or 0.4 (200–250 °C) mTorr of NH_3 . The thickness of the measured films ranges from 26 to 32 nm.

at 150–200 °C, $\text{MoC}_{0.32}\text{N}_{0.27}$ at 250 °C, and $\text{MoC}_{0.12}\text{N}_{0.40}$ at 300 °C (Fig. 2). Increasing the temperature also increases the growth rate: At 0.01 mTorr of $\text{Mo}(\text{CO})_6$ and 0.4 mTorr of NH_3 , the growth rate is 0.4, 1.2, and 2 nm/min at 150, 200, and 250 °C, respectively.

B. Film properties

Cross-sectional SEM micrographs indicate that the MoC_xN_y films are smooth, dense, and featureless; a 25 nm thick film grown at 150 °C has an rms roughness of only 1.1 nm. The room temperature resistivities are 200–300 $\mu\Omega$ cm, and there was no clear trend for resistivity as a function of growth conditions. Films grown at 150 °C from 0.01 mTorr of $\text{Mo}(\text{CO})_6$ and 0.7 mTorr of NH_3 have a T_c of 4.7 K. For films grown at an increased NH_3 pressure of 1.3 mTorr at the same growth temperature, the resistance starts to decrease around 6 K, but zero resistance is not observed down to 4 K. We attribute this latter behavior to the existence of a second non-superconducting phase, as evidenced by XRD data discussed next. For films grown from 0.01 mTorr of $\text{Mo}(\text{CO})_6$ and 0.4 mTorr of NH_3 , the superconducting transition occurs at

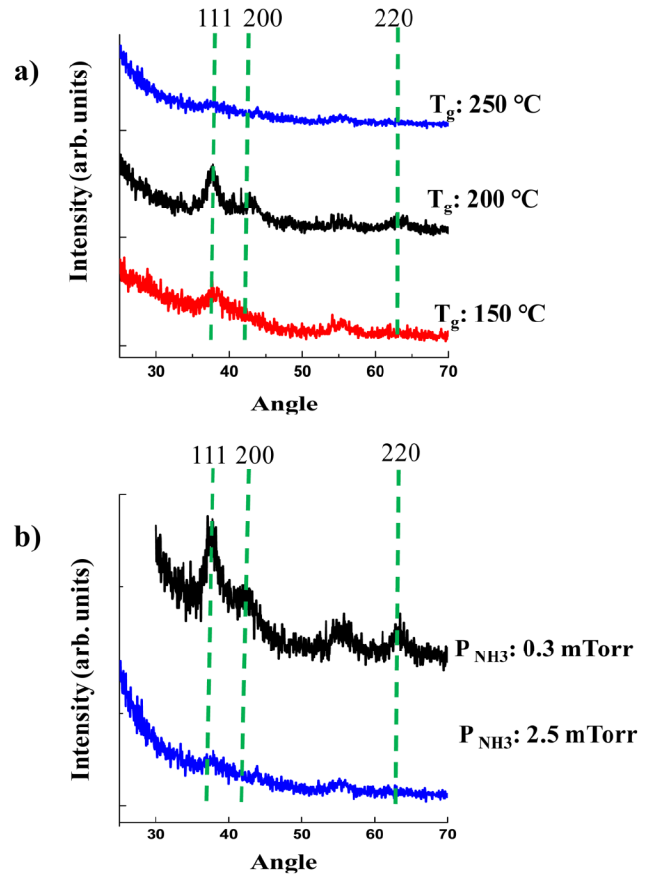


FIG. 4. (a) GIXRD pattern of superconducting molybdenum carbonitride films grown at substrate temperatures of 150–250 °C with 2.5 mTorr of NH_3 . Peak positions at 150 and 200 °C are consistent with cubic Mo_2C and Mo_2N (which have very similar lattice constants); the film grown at 250 °C is apparently amorphous. (b) GIXRD pattern of molybdenum carbonitride films grown at 250 °C with 2.5 mTorr of NH_3 (the same data as in a) or 0.3 mTorr of NH_3 ; peak assignments are the same as in part (a).

4.5 K for films grown at 200 °C and at 5.2 K for films grown at 250 °C (Fig. 3). Comparable resistivities at low temperature and room temperature indicate disorder, residual resistivity ratio (RRR) ~ 1 .

The films grown at 150–200 °C produce GIXRD peaks characteristic of (111), (200), and (220) reflections of the cubic phases $\gamma\text{-Mo}_2\text{N}$ and $\delta\text{-Mo}_2\text{C}$, whereas films grown at 250 °C appear amorphous [Fig. 4(a)].^{26,27} (The broad peak at $\sim 56^\circ$ is due to the Si substrate.)⁴⁰ However, distinction of the nitride and carbide phases is not possible because the 3% difference in cell constants falls within the $\sim 2^\circ\text{--}3^\circ$ line widths of the diffraction peaks. The films may be carbonitride solid solutions. The Scherrer formula applied to the (111) peak estimates an average grain diameter of 2 and 5 nm for films grown at 150 and 200 °C, respectively; however, the precision is limited by the low signal-to-noise and difficult to distinguish nitride and carbide phases. At a growth temperature of 250 °C, increasing the NH_3 pressure results in broader x-ray peaks and a more dominant amorphous background, suggesting that nitrogen concentration reduces crystallinity [Fig. 4(b)]. The increased N content or the decreased crystallinity may be responsible for the loss of superconductivity¹⁶ when NH_3 pressure was increased from 0.7 to 1.3 mTorr at 150 °C; we note, however, that some studies report an increase in T_c with disorder [see $\gamma\text{-Mo}_2\text{N}$ in Table I (Refs. 14–16)]. Diffraction patterns for films grown at 300 °C from 0.01 mTorr $\text{Mo}(\text{CO})_6$ and either 0.3 or

9 mTorr NH_3 exhibit the same peaks as those grown at lower temperatures [Fig. 4(a)].

C. Film conformality

The conformal (step) coverage in trench structures with a depth:width (aspect) ratio of 6:1 is very good: the coverage is 0.85 when the films are grown at 150 °C from 0.01 mTorr of $\text{Mo}(\text{CO})_6$ and 1.3 mTorr of NH_3 [Fig. 5(a)] and 0.80 when grown at 200 °C from 0.01 mTorr of $\text{Mo}(\text{CO})_6$ and 0.4 mTorr of NH_3 (the latter conditions afford superconducting films with $T_c = 4.5$ K) [Fig. 5(b)]. These step coverages, which are reasonably high, were achieved by employing gas delivery lines that are pointed toward the substrate. Recent work, including calculation of ballistic particle transport in trench structures, shows that forward-directed flux from similarly arranged gas delivery lines greatly improves step coverage, and it can even create superconformal (bottom-up) coating profiles under suitable conditions.⁴¹

IV. CONCLUSIONS

Low temperature CVD is used to deposit thin films of molybdenum carbonitride from $\text{Mo}(\text{CO})_6$ and NH_3 in the temperature range 150–300 °C. Film compositions of $\text{MoC}_{0.48}\text{N}_{0.2}$ to $\text{MoC}_{0.36}\text{N}_{0.33}$ are achieved by increasing the NH_3 pressure from 0.3 to 3.3 mTorr at a constant $\text{Mo}(\text{CO})_6$ pressure of 0.01 mTorr and a substrate temperature of 200 °C. At a constant $\text{Mo}(\text{CO})_6$ pressure of 0.01 mTorr and an NH_3 pressure of 2 mTorr, the composition is $\sim\text{MoC}_{0.5}\text{N}_{0.3}$ from 150 to 200 °C, $\text{MoC}_{0.32}\text{N}_{0.27}$ at 250 °C, and $\text{MoC}_{0.12}\text{N}_{0.40}$ at 300 °C. Superconducting critical temperatures of 4.7, 4.5, and 5.2 K are reported for films grown at 150, 200, and 250 °C, respectively. Films are highly conformal in trenches of aspect ratio 6:1 and are composed of nanocrystalline grains of one or a mixture of cubic Mo_2C and Mo_2N phases; the high step coverages are attributed to the use of a low pressure CVD apparatus in which the flux of precursor to the surface is forward-directed.

ACKNOWLEDGMENTS

Financial support from MIT-Lincoln Laboratories is gratefully acknowledged. G.S.G. acknowledges support from the National Science Foundation (NSF) under Grant No. CHE 1665191. J.R.A. acknowledges support from the National Science Foundation under Grant No. DMR 1410209.

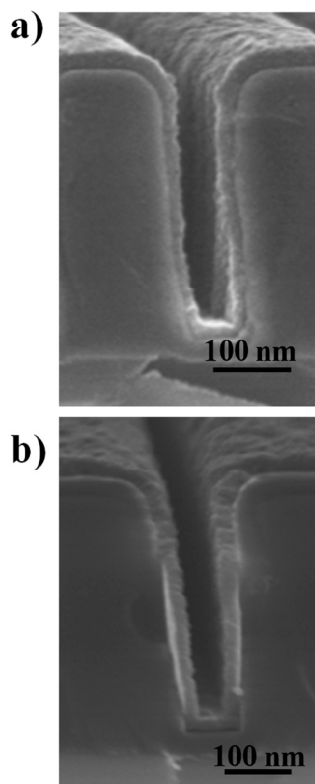


FIG. 5. Cross-sectional SEM micrographs of trenches with aspect ratio 6:1 coated conformally with molybdenum carbonitride at (a) 150 °C and (b) 200 °C.

¹Y. Jang *et al.*, *J. Alloys Compd.* **663**, 651 (2016).

²Y. He and J. Y. Feng, *J. Cryst. Growth* **263**, 203 (2004).

³J. Danroc, A. Aubert, and R. Gillet, *Thin Solid Films* **153**, 281 (1987).

⁴J. Valli, U. Mäkelä, and H. T. G. Hentzell, *J. Vac. Sci. Technol. A* **4**, 2850 (1986).

⁵H. Peter, M. Nicolas, R. Manfred, and L. Francis, *J. Phys. D Appl. Phys.* **36**, 1023 (2003).

⁶S. Wang, D. Antonio, X. Yu, J. Zhang, A. L. Cornelius, D. He, and Y. Zhao, *Sci. Rep.* **5**, 13733 (2015).

⁷K. S. Lee, H. Abe, J. A. Reimer, and A. T. Bell, *J. Catal.* **139**, 34 (1993).

⁸T. Kadono, T. Kubota, and Y. Okamoto, *Catal. Today* **87**, 107 (2003).

⁹S. Gong, H. Chen, W. Li, B. Li, and T. Hu, *J. Mol. Catal. A Chem.* **225**, 213 (2005).

¹⁰R. Kojima and K.-i. Aika, *Appl. Catal. A Gen.* **219**, 141 (2001).

¹¹I. Jauberteau, A. Bessadou, R. Mayet, J. Cornette, J. L. Jauberteau, P. Carles, and T. Merle-Mejean, *Coatings* **5**, 656 (2015).

¹²D. A. Papaconstantopoulos, W. E. Pickett, B. M. Klein, and L. L. Boyer, *Phys. Rev. B Condens. Matter* **31**, 752 (1985).

¹³N. Savvides, *J. Appl. Phys.* **62**, 600 (1987).

¹⁴G. Linker, R. Smithey, and O. Meyer, *J. Phys. F Met. Phys.* **14**, L115 (1984).

¹⁵R. Baskaran, A. V. Thanikai Arasu, E. P. Amaladass, L. S. Vaidhyanathan, and D. K. Baisnab, *J. Phys. D Appl. Phys.* **49**, 205304 (2016).

¹⁶H. Luo *et al.*, *J. Phys. Chem. C* **115**, 17880 (2011).

¹⁷A. Y. Ganin, L. Kienle, and G. V. Vajenine, *J. Solid State Chem.* **179**, 2339 (2006).

¹⁸A. Bezinge, K. Yvon, J. Muller, W. Lengaeur, and P. Ettmayer, *Solid State Commun.* **63**, 141 (1987).

¹⁹K. Yamaura, Q. Huang, M. Akaishi, and E. Takayama-Muromachi, *Phys. Rev. B* **74**, 184510 (2006).

²⁰N. Morton, B. W. James, G. H. Wostenholm, D. G. Pomfret, M. R. Davies, and J. L. Dykins, *J. Less-Common. Met.* **25**, 97 (1971).

²¹N. S. Athanasiou, *Mod. Phys. Lett. B* **11**, 939 (1997).

²²C. I. Sathish *et al.*, *J. Solid State Chem.* **196**, 579 (2012).

²³V. Sadagapan and H. C. Gatos, *J. Phys. Chem. Solids* **27**, 235 (1966).

²⁴M. K. Kolel-Veetil, S. B. Qadri, M. Osofsky, and T. M. Keller, *Chem. Mater.* **17**, 6101 (2005).

²⁵A. Yanguas-Gil, Y. Yang, N. Kumar, and J. R. Abelson, *Surf. Films* **27**, 1235 (2009).

²⁶H.-T. Chiu, W.-Y. Ho, and S.-H. Chuang, *J. Mater. Res.* **9**, 1622 (2011).

²⁷A. Bertuch, B. D. Keller, N. Ferralis, J. C. Grossman, and G. Sundaram, *J. Vac. Sci. Technol. A* **35**, 01B141 (2016).

²⁸D. K. Nandi, U. K. Sen, D. Choudhury, S. Mitra, and S. K. Sarkar, *ACS Appl. Mater. Interfaces* **6**, 6606 (2014).

²⁹S. Jayaraman, Y. Yang, D. Y. Kim, G. S. Girolami, and J. R. Abelson, *J. Vac. Sci. Technol. A* **23**, 1619 (2005).

³⁰R. Fix, R. G. Gordon, and D. M. Hoffman, *Chem. Mater.* **5**, 614 (1993).

³¹S. Babar, N. Kumar, P. Zhang, J. R. Abelson, A. C. Dunbar, S. R. Daly, and G. S. Girolami, *Chem. Mater.* **25**, 662 (2013).

³²S. Babar, T. T. Li, and J. R. Abelson, *J. Vac. Sci. Technol. A* **32**, 060601 (2014).

³³M.-H. Lo and W.-C. J. Wei, *J. Am. Ceram. Soc.* **80**, 886 (1997).

³⁴M. Kmetz, S. L. Suib, and F. S. Galasso, *J. Am. Ceram. Soc.* **72**, 1523 (1989).

³⁵W. C. J. Wei and M. H. Lo, *Appl. Organomet. Chem.* **12**, 201 (1998).

³⁶R. F. Howe, D. E. Davidson, and D. A. Whan, *J. Chem. Soc. Faraday Trans. 1 Phys. Chem. Condens. Phases* **68**, 2266 (1972).

³⁷W. Zheng *et al.*, *J. Am. Chem. Soc.* **135**, 3458 (2013).

³⁸S. T. Oyama, *Catal. Today* **15**, 179 (1992).

³⁹J. S. J. Hargreaves, *Coordin. Chem. Rev.* **257**, 2015 (2013).

⁴⁰C. Weiss, M. Rumpel, M. Schnabel, P. Loper, and S. Janz, presented at the European Photovoltaic Solar Energy Conference and Exhibition, Paris, France, 2013 (unpublished).

⁴¹T. K. Talukdar, W. B. Wang, G. S. Girolami, and J. R. Abelson, *J. Vac. Sci. Technol. A* **36**, 051513 (2018).

⁴²See supplementary material at <https://doi.org/10.1116/1.5079805> for high resolution XPS results for one molybdenum carbonitride film.